

# Solid-State Intermetallic Compound Layer Growth Between Copper and 95.5Sn-3.9Ag-0.6Cu Solder

PAUL T. VIANCO,<sup>1,2</sup> JEROME A. REJENT,<sup>1</sup> and PAUL F. HLAVA<sup>1</sup>

1.—Sandia National Laboratories, Albuquerque, NM 87185. 2.—E-mail: ptvianco@sandia.gov

Long-term, solid-state intermetallic compound (IMC) layer growth was examined in 95.5Sn-3.9Ag-0.6Cu (wt.%) /copper (Cu) couples. Aging temperatures and times ranged from 70°C to 205°C and from 1 day to 400 days, respectively. The IMC layer thicknesses and compositions were compared to those investigated in 96.5Sn-3.5Ag/Cu, 95.5Sn-0.5Ag-4.0Cu/Cu, and 100Sn/Cu couples. The nominal Cu<sub>3</sub>Sn and Cu<sub>6</sub>Sn<sub>5</sub> stoichiometries were observed. The Cu<sub>3</sub>Sn layer accounted for 0.4–0.6 of the total IMC layer thickness. The 95.5Sn-3.9Ag-0.6Cu/Cu couples exhibited porosity development at the Cu<sub>3</sub>Sn/Cu interface and in the Cu<sub>3</sub>Sn layer as well as localized “plumes” of accelerated Cu<sub>3</sub>Sn growth into the Cu substrate when aged at 205°C and  $t > 150$  days. An excess of 3–5at.%Cu in the near-interface solder field likely contributed to IMC layer growth. The growth kinetics of the IMC layer in 95.5Sn-3.9Ag-0.6Cu/Cu couples were described by the equation  $x = x_0 + At^n \exp[-\Delta H/RT]$ . The time exponents,  $n$ , were  $0.56 \pm 0.06$ ,  $0.54 \pm 0.07$ , and  $0.58 \pm 0.07$  for the Cu<sub>3</sub>Sn layer, the Cu<sub>6</sub>Sn<sub>5</sub>, and the total layer, respectively, indicating a diffusion-based mechanism. The apparent-activation energies ( $\Delta H$ ) were Cu<sub>3</sub>Sn layer:  $50 \pm 6$  kJ/mol; Cu<sub>6</sub>Sn<sub>5</sub> layer:  $44 \pm 4$  kJ/mol; and total layer:  $50 \pm 4$  kJ/mol, which suggested a fast-diffusion path along grain boundaries. The kinetics of Cu<sub>3</sub>Sn growth were sensitive to the Pb-free solder composition while those of Cu<sub>6</sub>Sn<sub>5</sub> layer growth were not so.

**Key words:** Pb-free solder, intermetallic compound layer, solid-state growth, copper

## INTRODUCTION

The implementation of Pb-free solders continues in electronic assemblies. Copper (Cu) will remain as the predominant substrate material to which will be made second and third level soldered interconnections. During the assembly process, the molten solder reacts with Cu, resulting in (1) Cu dissolution into the solder and (2) the development of an intermetallic compound (IMC) layer at the solder/Cu interface. The extent of Cu dissolution is dependent upon the molten solder temperature, the time interval, and the composition of the solder. The resulting IMC layer is typically 1–2- $\mu\text{m}$  thick.<sup>1,2</sup> The IMC layer can continue to develop at the interface after solidification via thermally activated, solid-state diffusion mechanisms. The solid-state IMC layer growth con-

sumes the solder and the Cu substrate, potentially impacting both solderability as well as the long-term reliability of the interconnections.

Solid-state IMC layer growth has been investigated for several Sn-containing solders on Cu including the following couples: 63Sn-37Pb/Cu (wt.%), 100Sn/Cu, 96.5Sn-3.5Ag/Cu, 95.5Sn-0.5Ag-4.0Cu/Cu, 95Sn-5Sb/Cu, 91.84Sn-3.33Ag-4.83Bi/Cu, and 58Bi-42Sn/Cu.<sup>3–7</sup> The cited studies documented the composition and growth kinetics of the IMC layers that developed at the solder/Cu interface.

Those studies provided insight into the role of solder composition on the physical metallurgy and kinetics of solid-state, interfacial IMC layer growth. For example, the IMC layer will simply grow around Ag<sub>3</sub>Sn particles that are present in the 96.5Sn-3.5Ag solder of couples made to Cu (Fig. 1). On the other hand, a solute element present in the Sn-rich phase is often rejected ahead of the IMC layer. This

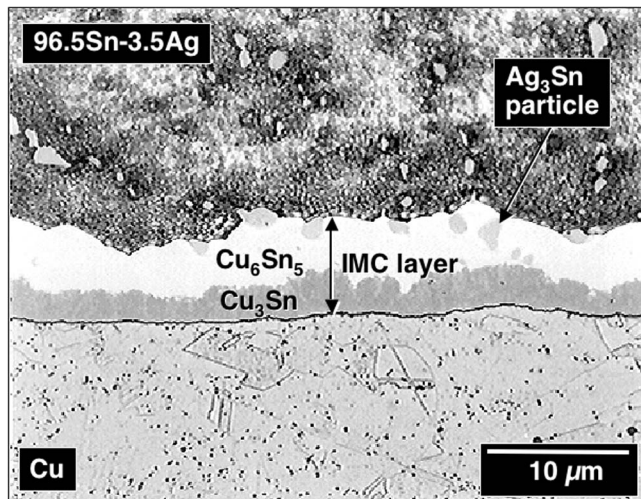


Fig. 1. Optical micrograph showing IMC layer growth around  $\text{Ag}_3\text{Sn}$  particles present in the solder of the 96.5Sn-3.5Ag/Cu couple aged at 170°C for 200 days.

process results in the Pb-rich layer that develops ahead of the Cu-Sn IMC layer that forms in 63Sn-37Pb/Cu couples (Fig. 2a). In 58Bi-42Sn solder/Cu couples, rapid solid-state IMC layer growth resulted in the formation of Bi-rich bands within the IMC layer (Fig. 2b).<sup>5</sup> The incorporated Bi actually altered the Cu-Sn stoichiometry away from the usual  $\text{Cu}_6\text{Sn}_5$  composition.

A feature of solid-state IMC layer development between Sn-based solders and Cu substrates is that the appearance of the  $\text{Cu}_3\text{Sn}$  stoichiometry between the Cu substrate and the traditionally observed,  $\text{Cu}_6\text{Sn}_5$  stoichiometry is sensitive to the solder composition. The extent of  $\text{Cu}_3\text{Sn}$  formation can be expressed by the ratio of  $\text{Cu}_3\text{Sn}$  thickness to the total layer thickness ( $\text{Cu}_3\text{Sn} + \text{Cu}_6\text{Sn}_5$ ). The ratio values, along with the aging conditions under which the

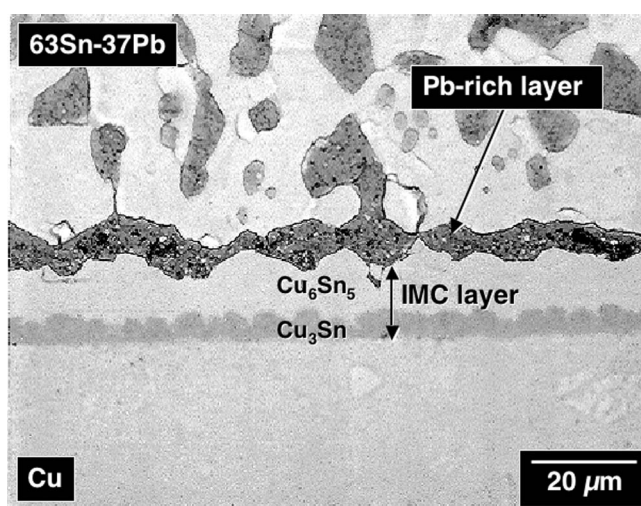
$\text{Cu}_3\text{Sn}$  layer appeared, are listed in Table I for several solder/Cu couples. The first appearance of the  $\text{Cu}_3\text{Sn}$  layer depends upon the solder composition. For example, the  $\text{Cu}_3\text{Sn}$  layer was present in 95.5Sn-0.5Ag-4.0Cu/Cu couples at all of the aging temperatures. On the other hand, aging temperatures greater than or equal to 170°C were required to generate the  $\text{Cu}_3\text{Sn}$  layer in 96.5Sn-3.5Ag/Cu couples. Despite the unique behavior of the  $\text{Cu}_3\text{Sn}$  layer shown in Table I, nearly identical, total IMC layer thicknesses ( $\text{Cu}_3\text{Sn} + \text{Cu}_6\text{Sn}_5$ ) were documented for the three solder compositions.

Of particular interest to the present study was the effect of the nominal, solder Cu content on solid-state IMC layer development. A previous study examined 95.5Sn-0.5Ag-4.0Cu/Cu couples.<sup>7</sup> It was observed that these couples exhibited less IMC layer thickness fluctuations when compared to similar data from 63Sn-37Pb/Cu, 96.5Sn-3.5Ag/Cu, and 95Sn-5Sb/Cu couples. This trend was likely a consequence of the elevated Cu content. The  $\text{Cu}_6\text{Sn}_5$  particles contained in the solder field did not physically impede IMC layer growth because a depletion zone of such particles formed near the solder/IMC layer interface. That zone is illustrated by scanning electron microscopy (SEM) photographs in Fig. 3 that show two conditions: (a) 100°C, 25 days having no depletion zone and (b) 205°C, 40 days where the zone is extensive. However, the  $\text{Cu}_6\text{Sn}_5$  particles in the near solder field may have indirectly affected IMC layer growth.

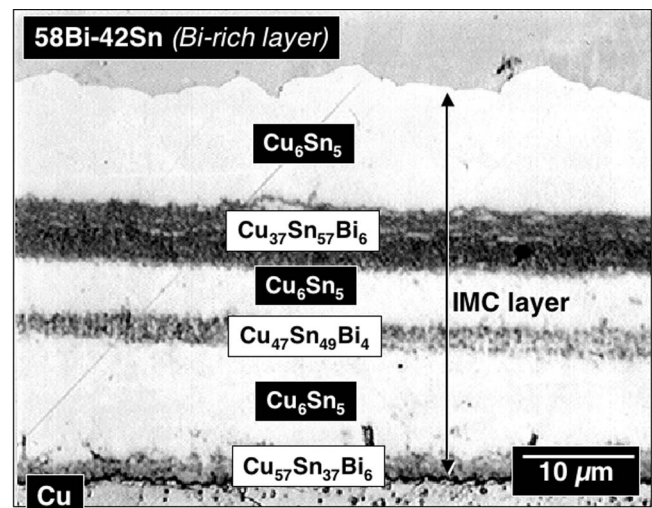
Solid-state aging studies of solder/Cu couples have described the IMC layer growth-rate kinetics according to Eq. 1:

$$x = x_0 + A t^n \exp(-\Delta H/RT) \quad (1)$$

where  $x$  is the layer thickness (m) at time  $t$  (sec);  $x_0$  is the initial layer thickness (m);  $n$  is the time expo-



a



b

Fig. 2. (a) Optical micrograph showing the Pb-rich layer at the solder/IMC layer interface of a 63Sn-37Pb/Cu couple aged at 135°C for 400 days. (b) Optical micrograph showing the banded structure caused by the incorporation of Bi in the IMC layer in a 58Bi-42Sn ( $T_{\text{eut}} = 139^\circ\text{C}$ )/Cu couple that was aged at 120°C for 400 days.

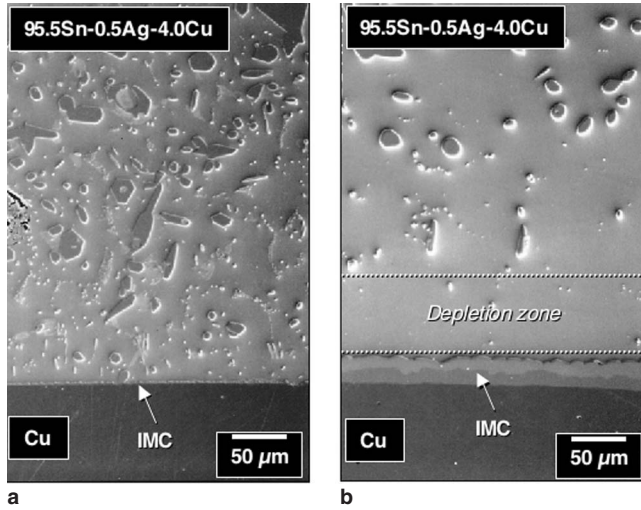


Fig. 3. The SEM photographs show formation of a  $\text{Cu}_6\text{Sn}_5$  particle-depletion zone in 95.5Sn-0.5Ag-4.0Cu/Cu couples that was caused by solid-state IMC layer growth: (a) minimal aging, 100°C, 25 days and (b) extensive aging, 205°C, 40 days.

ment;  $\Delta H$  is the apparent-activation energy (kJ/mol);  $R$  is the universal gas constant, 8.314 J/mol-K; and  $T$  is temperature (K). Equation 1 was reformatted by taking the logarithm of both sides, resulting in Eq. 2:

$$\ln(x - x_0) = \ln(A) + n \ln(t) - \Delta H/RT \quad (2)$$

A multivariable linear regression analysis was performed on the data according to Eq. 2. The independent variables were  $\ln(t)$  and  $1/T$ ; the dependent variable was  $\ln(x - x_0)$ . The regression analysis returned the coefficients  $\ln(A)$ ,  $n$ , and  $\Delta H/R$  from which the respective kinetics parameters  $A$ ,  $n$ , and  $\Delta H$  were determined.

Shown in Tables II–IV are the kinetics parameters for growth of the  $\text{Cu}_3\text{Sn}$  layer, the  $\text{Cu}_6\text{Sn}_5$  layer, and the total IMC layer ( $\text{Cu}_3\text{Sn} + \text{Cu}_6\text{Sn}_5$  thicknesses), respectively, of the following couples: 100Sn/Cu, 95.5Sn-0.5Ag-4.0Cu/Cu, and 96.5Sn-3.5Ag/Cu. (A similar compilation of solid-state IMC growth-kinetics parameters for other Pb-free solders can be found in Ref. 8. The error terms represent 95% confidence intervals. Common to each of the solders was an absence of the  $\text{Cu}_3\text{Sn}$  layer in the as-fabricated couples ( $x_0 = 0$ ). Second, the values of the time exponent,  $n$ , were generally similar to 0.5, indicating that solid-state diffusion was responsible for growth of the  $\text{Cu}_3\text{Sn}$  and  $\text{Cu}_6\text{Sn}_5$  layers (and total IMC layer).<sup>9</sup> The noted exceptions were  $\text{Cu}_3\text{Sn}$ -layer growth in 100Sn/Cu and 95.5Sn-0.5Ag-4Cu/Cu couples. The values of the apparent-activation energy were statistically in the range of 40–60 kJ/mol, with the same

Table I. Ratio  $\text{Cu}_3\text{Sn}/(\text{Cu}_3\text{Sn} + \text{Cu}_6\text{Sn}_5)$  Resulting from Solid-State IMC Layer Growth

Composition (wt.%)	Aging	Aging Time (days) Temperature (°C)	Ratio $\text{Cu}_3\text{Sn}/(\text{Cu}_3\text{Sn} + \text{Cu}_6\text{Sn}_5)$
100Sn	70	25–350	1
	100	10–100	1
	100	200–350	0.50–0.55
	135	10–25	0.60
	135	100–400	0.33
	170	100–400	0.55
	205	100–200	0.55
95.5Sn-0.5Ag-4Cu	70	200–400	0–0.28
	100	100–350	0.50–0.60
	135	10–350	0.53
	170	10–300	0.40–0.60
	205	10–300	0.40–0.60
96.5Sn-3.5Ag	170	10–400	0.20–0.45
	205	10–200	0.20–0.45

Table II. Solid-State Growth-Kinetics Parameters for the  $\text{Cu}_3\text{Sn}$  Layer

Composition (wt.%)	$x_0$ (m)	$A$ ( $\text{m}\cdot\text{s}^{1/n}$ )	$n$	$\Delta H$ (kJ/mol)
100Sn	0	$1.18 \times 10^{-4}$	$0.33 \pm 0.06$	$29 \pm 4$
95.5Sn-0.5Ag-4Cu	0	$4.64 \times 10^{-4}$	$0.39 \pm 0.05$	$38 \pm 3$
96.5Sn-3.5Ag	0	$6.14 \times 10^{-5}$	$0.58 \pm 0.30$	$42 \pm 40$

Table III. Solid-State Growth-Kinetics Parameters for the  $\text{Cu}_6\text{Sn}_5$  Layer

Composition (wt.%)	$x_0$ (m)	$A$ ( $\text{m}\cdot\text{s}^{1/n}$ )	$n$	$\Delta H$ (kJ/mol)
100Sn	$0.79 \times 10^{-6}$	$1.18 \times 10^{-5}$	$0.54 \pm 0.06$	$35 \pm 16$
95.5Sn-0.5Ag-4Cu	$1.70 \times 10^{-6}$	$1.56 \times 10^{-3}$	$0.47 \pm 0.09$	$49 \pm 5$
96.5Sn-3.5Ag	$1.83 \times 10^{-6}$	$4.19 \times 10^{-3}$	$0.46 \pm 0.12$	$50 \pm 8$

**Table IV. Solid-State Growth-Kinetics Parameters for the Total IMC Layer (Cu<sub>3</sub>Sn + Cu<sub>6</sub>Sn<sub>5</sub>)**

Composition (wt.%)	$x_0$ (m)	A (m·s <sup>-1/n</sup> )	n	ΔH (kJ/mol)
100Sn	$0.79 \times 10^{-6}$	$1.47 \times 10^{-2}$	$0.46 \pm 0.16$	$53 \pm 9$
95.5Sn-0.5Ag-4Cu	$1.70 \times 10^{-6}$	$1.72 \times 10^{-2}$	$0.52 \pm 0.08$	$58 \pm 5$
96.5Sn-3.5Ag	$1.83 \times 10^{-6}$	$2.04 \times 10^{-2}$	$0.50 \pm 0.12$	$57 \pm 8$

preceding exceptions. These values of ΔH can be attributed to so-called fast-diffusion processes, most likely atomic transport along grain boundaries in the IMC layer.<sup>10</sup> The data in Tables II–IV, along with the ratio metrics in Table I, provided benchmarks against which to compare the solid-state IMC layer growth of the 95.5Sn-3.9Ag-0.6Cu solder on Cu.

### EXPERIMENTAL PROCEDURES

The substrate material was oxygen-free, high conductivity Cu pieces having dimensions of 6.35 mm × 6.35 mm × 1.59 mm. The surface that was used for the IMC layer analysis was polished to a 0.05-μm alumina finish. The composition of the solder was 95.5Sn-3.9Ag-0.6Cu (wt.%), which was certified by the manufacturer's documentation. The Cu piece was coated with a water-soluble flux and subsequently immersed into a bath of molten 95.5Sn-3.9Ag-0.6Cu solder for 5 sec. The solder temperature was 260°C. The piece was withdrawn from the bath with the polished surface facing down in order to provide an "infinite" solder quantity for IMC layer development.

Accelerated aging was performed in air furnaces with a temperature control of ±0.5°C. The aging temperatures were 70°C, 100°C, 135°C, 170°C, and 205°C. The aging times ranged from 1 day to 400 days with a tracking accuracy of ±30 min. Upon completion of the aging treatment, the Cu piece was cross-sectioned along one of the diagonals. One of the halves was mounted, edge-on, in cold setting epoxy for metallographic sample-preparation procedures.

The IMC layer thickness was determined using the following procedure. Four locations were selected along the solder/Cu interface. At each location, a 1,000× magnification, digitized optical micrograph was taken of the IMC layer. Thickness measurements were performed at 13 equally spaced locations on each micrograph, using an image analysis procedure. When present, the Cu<sub>3</sub>Sn-layer thickness was measured directly, as was the total IMC layer thickness. The thickness of the Cu<sub>6</sub>Sn<sub>5</sub> layer was determined by the difference between the Cu<sub>3</sub>Sn and total IMC layer thickness values. In the absence of a Cu<sub>3</sub>Sn layer, the Cu<sub>6</sub>Sn<sub>5</sub> layer thickness was measured directly. The thickness values were represented by a mean and an error term of ± one standard deviation.

Electron probe microanalysis (EPMA) was used to determine the composition of the IMC layer. The operating voltage was 15 keV, resulting in an x-ray sampling-volume diameter of 1–2 × 10<sup>-6</sup> m. Five traces were performed across the solder/Cu interface using 1 × 10<sup>-6</sup> m steps. The samples that were evaluated by EPMA were exposed to the following

aging conditions: as-fabricated; 70°C, 25 days and 200 days; 100°C, 25 days, 200 days, and 400 days; 135°C, 200 days; 170°C, 200 days; and 205°C, 10 days, 50 days, 200 days, and 400 days.

### RESULTS AND DISCUSSION

The total IMC layer thickness of the as-fabricated sample was  $0.9 \pm 0.3 \times 10^{-6}$  m. This value was comparable to the initial thickness of 100Sn/Cu couples. However, it was approximately one-half of those measured for the 96.5Sn-3.5Ag/Cu and 95.5Sn-0.5Ag-4Cu/Cu couples (Tables III and IV).

Solid-state aging resulted in further growth of the IMC layer. Shown in Fig. 4 are representative optical micrographs of the IMC layer morphology after aging at 170°C for (a) 150 days and (b) 300 days. The total IMC layer was comprised of the individual Cu<sub>3</sub>Sn and Cu<sub>6</sub>Sn<sub>5</sub> layers.\* The IMC layer thickness data were categorized into two temperature regimes. There was a low-temperature regime defined by data taken at 70°C, 100°C, and 135°C and a high-temperature regime that included the 170°C and 205°C data. The reason for this categorization approach will be discussed later.

#### The 95.5Sn-3.9Ag-0.6Cu/Cu IMC Layer Growth at 70°C, 100°C, and 135°C

The total IMC layer thickness as a function of aging time is shown in Fig. 5 for the three temperatures. Only the Cu<sub>6</sub>Sn<sub>5</sub> layer was present in couples aged at 70°C or 100°C and all time periods. The Cu<sub>3</sub>Sn layer appeared after aging at 135°C for times greater than or equal to 10 days. The individual curves for Cu<sub>3</sub>Sn and Cu<sub>6</sub>Sn<sub>5</sub> are also shown in Fig. 5. The Cu<sub>3</sub>Sn-layer thickness comprised approximately one-half of the total IMC layer thickness.

The IMC layer growth shown in Fig. 5 was compared to those of each of the 96.5Sn-3.5Ag/Cu, 95.5Sn-0.5Ag-4Cu/Cu, and 100Sn/Cu couples. The total IMC layer thicknesses of the 96.5Sn-3.5Ag/Cu couples aged at the same temperatures are shown in Fig. 6. Although only the Cu<sub>6</sub>Sn<sub>5</sub> stoichiometry was present, the thicknesses were comparable to those of the 95.5Sn-3.9Ag-0.6Cu/Cu couples (Fig. 5).

Shown in Fig. 7 is the total IMC layer thickness as a function of aging time for the 95.5Sn-0.5Ag-4Cu/Cu couples. The 70°C, 100°C, and 135°C aging temperatures produced a Cu<sub>3</sub>Sn layer at times greater than or equal to 350 days, 10 days, and 10 days, respectively. When present, the Cu<sub>3</sub>Sn layer accounted for

\* The precise stoichiometries were investigated in the EPMA portion of this study.

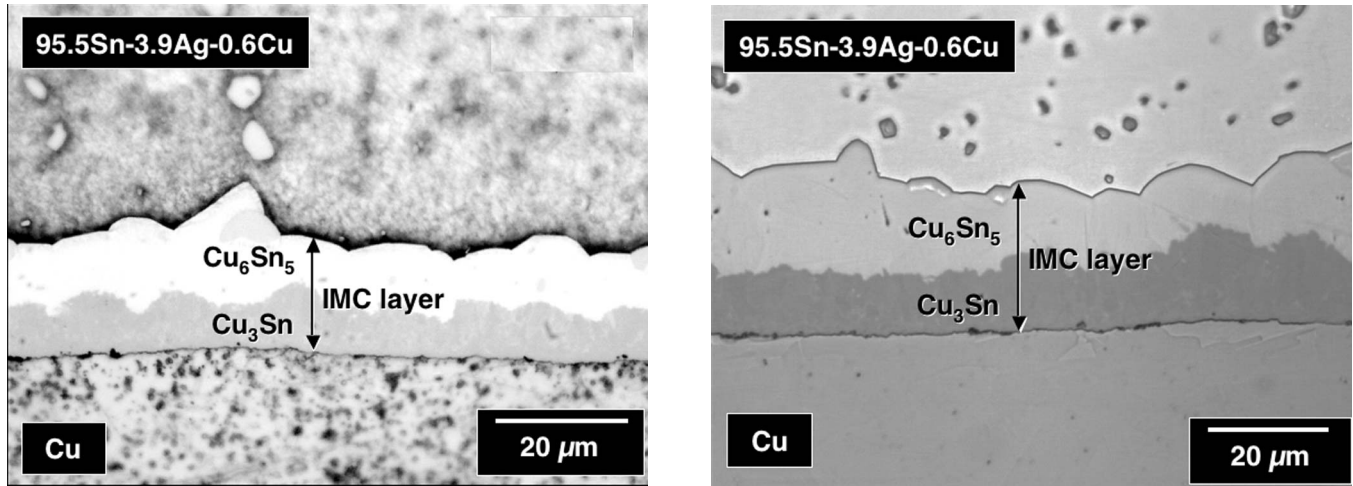


Fig. 4. Optical micrographs showing the development of the IMC layer in 95.5Sn-3.9Ag-0.6Cu/Cu couple after aging at 135°C for (a) 150 days and (b) 300 days. Both  $\text{Cu}_6\text{Sn}_5$  and  $\text{Cu}_3\text{Sn}$  layers were present.

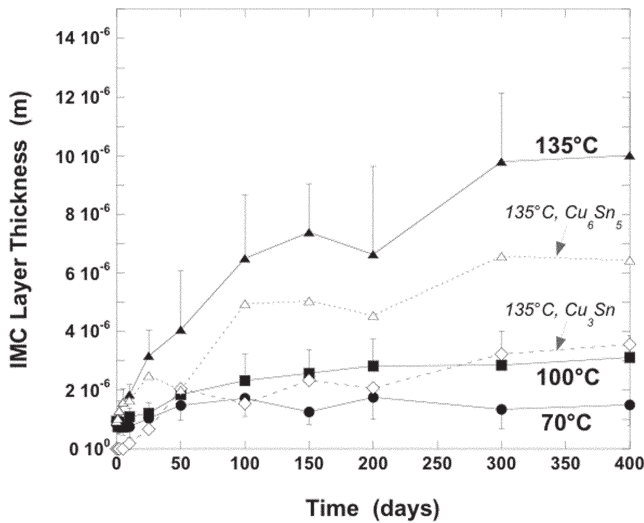


Fig. 5. Solid-state IMC-growth curves of total layer thickness from 95.5Sn-3.9Ag-0.6Cu/Cu couples aged at 70°C, 100°C, and 135°C. Also included are the individual  $\text{Cu}_3\text{Sn}$  and  $\text{Cu}_6\text{Sn}_5$  layer data that comprise the 135°C curve.

a 0.28–0.60 fraction of the total IMC layer thickness (Table I). In spite of the different layer morphology, the total IMC layer thicknesses of these couples were very similar to values measured with the 95.5Sn-3.9Ag-0.6Cu/Cu couples.

The total IMC layer thicknesses measured in 100Sn/Cu couples that were aged at 70°C, 100°C, and 135°C are presented in Fig. 8a. The 70°C and 100°C thicknesses were similar to those observed in the 95.5Sn-3.9Ag-0.6Cu/Cu couples for the same aging temperatures. However, unlike the 95.5Sn-3.9Ag-0.6Cu/Cu couples, the 100Sn/Cu couples developed only a  $\text{Cu}_3\text{Sn}$  layer at these two aging temperatures (Table I). The 100Sn/Cu couples exhibited an acceleration of IMC layer growth at 135°C that was accompanied by larger thickness fluctuations as indicated by the error bars in Fig. 8a and as illustrated by the optical micrograph in Fig. 8b. At aging times that

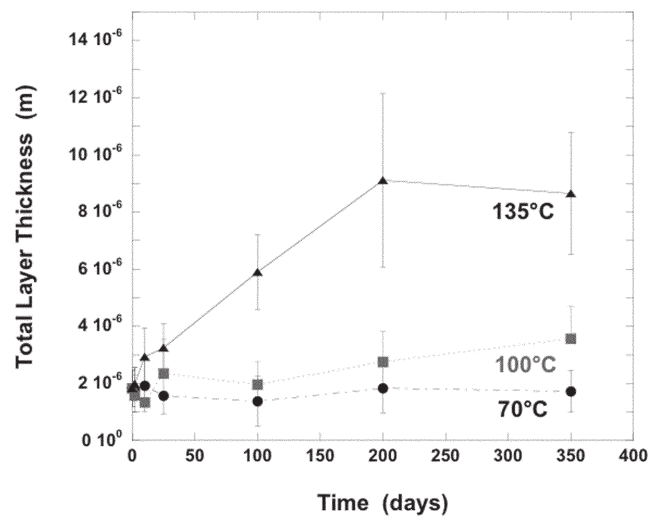


Fig. 6. Solid-state IMC-growth curves of total layer thickness from 96.5Sn-3.5Ag/Cu couples aged at 70°C, 100°C, and 135°C.

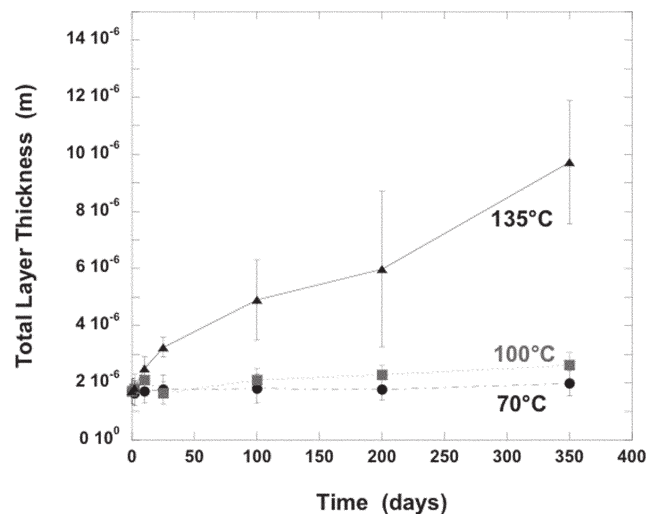
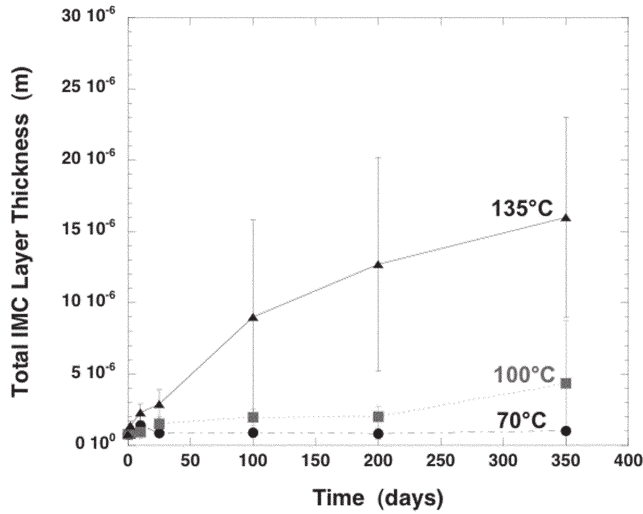
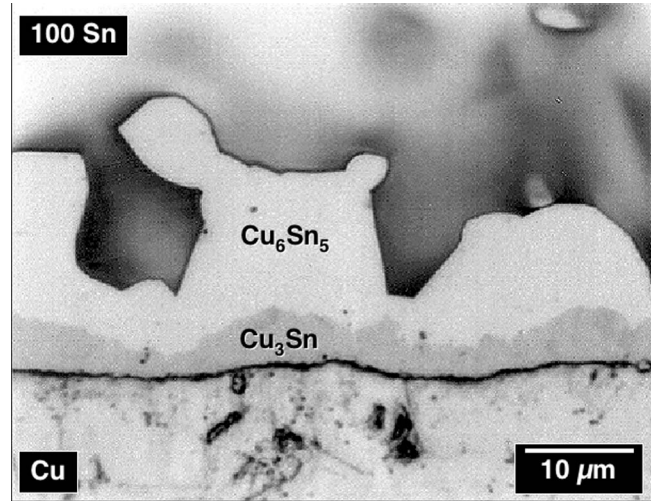


Fig. 7. Solid-state IMC-growth curves of the total layer thickness from 95.5Sn-0.5Ag-4.0Cu/Cu couples aged at 70°C, 100°C, and 135°C.



a



b

Fig. 8. (a) Solid-state IMC-growth curves of the total layer thickness from 100Sn/Cu couples aged at 70°C, 100°C, and 135°C. (b) Optical micrograph illustrates the large thickness variation that was observed in 100Sn/Cu couples aged at 135°C (shown is 200 days).

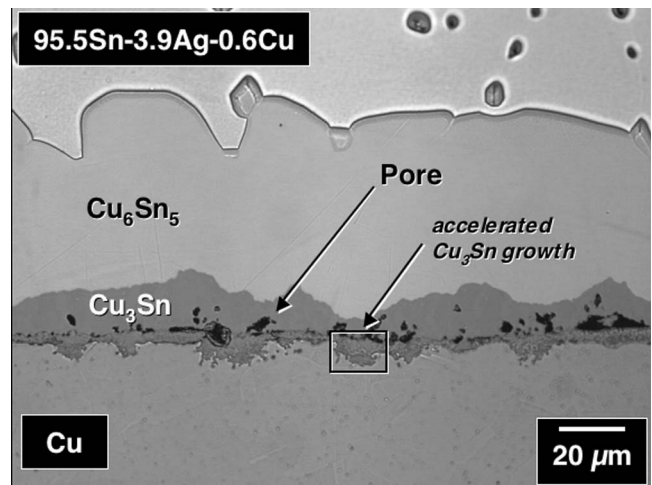
exceeded 100 days at 100°C and all times at 135°C, the  $\text{Cu}_3\text{Sn}$  stoichiometry comprised approximately one-half of the total IMC layer thickness in 100Sn/Cu couples.

In summary, solid-state aging of the 95.5Sn-3.9Ag-0.6Cu/Cu couples at 70°C, 100°C, and 135°C produced total IMC layer thicknesses that were similar to those of the other solder/Cu couples. The 95.5Sn-3.9Ag-0.6Cu/Cu couples required an aging temperature of 135°C to develop a measurable  $\text{Cu}_3\text{Sn}$  layer. However, once present, the  $\text{Cu}_3\text{Sn}$  layer accounted for a 0.4–0.6 fraction of the total IMC thicknesses. This range was similar to that of the other solders.†

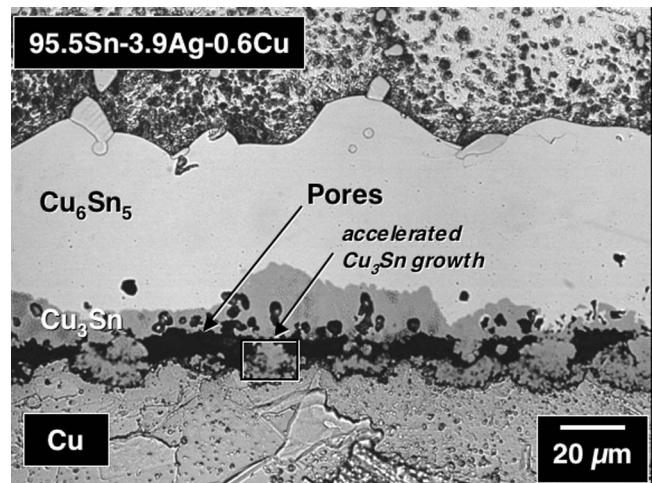
#### The 95.5Sn-3.9Ag-0.6Cu/Cu IMC Layer Growth at 170°C and 205°C

The  $\text{Cu}_3\text{Sn}$  layer appeared for all aging times at 170°C and 205°C. Unexpectedly, there was the development of porosity along the  $\text{Cu}_3\text{Sn}/\text{Cu}$  interface and, to a lesser extent, within the  $\text{Cu}_3\text{Sn}$  layer. Accompanying the porosity were localized regions or “plumes” of accelerated growth by the  $\text{Cu}_3\text{Sn}$  layer into the Cu substrate. These phenomena are illustrated by the optical micrographs in Fig. 9 that were taken of couples aged at 205°C for (a) 300 days and (b) 400 days. Initially, there were intermittent regions of very small pores that formed along the  $\text{Cu}_3\text{Sn}/\text{Cu}$  interface of couples aged at 170°C for time periods in excess of 150 days. The porosity increased in severity at the aging temperature of 205°C and time periods exceeding 150 days. Aging times in excess of 200 days (205°C) resulted in pore formation *within* the  $\text{Cu}_3\text{Sn}$  layer and accelerated

† In the case of the 63Sn-37Pb/Cu couples, the appearance of the  $\text{Cu}_3\text{Sn}$  stoichiometry occurred at aging times greater than or equal to 135 days at 135°C and 10 days at 170°C.<sup>3</sup> The layer was not observed at aging temperatures of 70°C and 100°C for time periods of up to 400 days. The  $\text{Cu}_3\text{Sn}$  layer comprised 0.2–0.4 of the total IMC layer.



a



b

Fig. 9. Optical micrographs showing porosity at the  $\text{Cu}_3\text{Sn}/\text{Cu}$  interface and in the  $\text{Cu}_3\text{Sn}$  layer of 95.5Sn-3.9Ag-0.6Cu/Cu couples aged at 205°C for (a) 300 days and (b) 400 days. Also evident are plumes of accelerated  $\text{Cu}_3\text{Sn}$  growth into the Cu substrate.

Cu<sub>3</sub>Sn growth into the Cu substrate (Fig. 9). These phenomena were *not* observed in the 100Sn/Cu, 96.5Sn-3.5Ag/Cu, or 95.5Sn-0.5Ag-4Cu/Cu couples under similar aging conditions.

The simultaneous presence of porosity and accelerated Cu<sub>3</sub>Sn formation into the Cu substrate suggested the occurrence of the Kirkendall effect. Unfortunately, the underlying driving force was not immediately apparent nor was the reason why that driving force was active only with 95.5Sn-3.9Ag-0.6Cu/Cu couples.

The IMC layer thickness data of 95.5Sn-3.9Ag-0.6Cu/Cu couples for the 170°C and 205°C aging temperatures were compared to those of the other solder/Cu couples in Fig. 10. (The 135°C data were included to overlap with the low-temperature regime.) Similar, total IMC layer thicknesses were observed between the solders for all aging times at 170°C (and 135°C), as shown in Fig. 10a. However, at 205°C and for aging times in excess of 50 days, total IMC layer growth accelerated in the 95.5Sn-3.9Ag-0.6Cu/Cu couples.

The aging temperature of 170°C produced similar Cu<sub>6</sub>Sn<sub>5</sub> and Cu<sub>3</sub>Sn-layer thicknesses between all of the solders (Fig. 10b and c). However, when aged at 205°C and times equal to or greater than 50 days, the 95.5Sn-3.9Ag-0.6Cu/Cu couples experienced a rapid increase in Cu<sub>6</sub>Sn<sub>5</sub> layer thickness (Fig. 10b). At aging times in excess of 150 days (205°C), the Cu<sub>3</sub>Sn-layer thickness had statistically stopped growing in 95.5Sn-3.9Ag-0.6Cu/Cu couples (Fig. 10c). The latter event coincided with the development of extensive porosity at the Cu<sub>3</sub>Sn/Cu interface (and layer in the Cu<sub>3</sub>Sn layer).

The following synopsis is drawn from the data in Fig. 10. All of the Pb-free solders exhibited similar IMC layer growth—total layer, Cu<sub>6</sub>Sn<sub>5</sub> layer, and Cu<sub>3</sub>Sn layer—at an aging temperature of 170°C (as well as at 135°C). The accelerated growth of the total IMC layer (Fig. 10a) in 95.5Sn-3.9Ag-0.6Cu/Cu couples exposed to 205°C for time periods in excess of 50 days was caused by a rapid growth of the Cu<sub>6</sub>Sn<sub>5</sub> layer (Fig. 10b). The Cu<sub>3</sub>Sn-layer thickness in 95.5Sn-3.9Ag-0.6Cu/Cu couples was similar to

those of the other solders when aged at 205°C for up to 150 days (Fig. 10c). At longer aging times, however, the Cu<sub>3</sub>Sn layer effectively stopped further growth. Coincident with the curtailment of Cu<sub>3</sub>Sn-layer growth was the formation of extensive porosity at the Cu<sub>3</sub>Sn/Cu interface and then in the Cu<sub>3</sub>Sn layer. It is important to note that accelerated growth of the Cu<sub>6</sub>Sn<sub>5</sub> layer *preceded* the halt of the Cu<sub>3</sub>Sn-layer growth and porosity formation, thereby implying a cause-and-effect between the two observations.

It was hypothesized that the rapid growth of the Cu<sub>6</sub>Sn<sub>5</sub> layer at 205°C drew more Cu from the substrate than the latter could re-supply at the Cu<sub>3</sub>Sn/Cu interface. As a result, porosity formed along the latter interface. The need for Cu by the Cu<sub>6</sub>Sn<sub>5</sub> layer was so extreme that Cu was then depleted from the Cu<sub>3</sub>Sn layer, causing the latter to stop growing and to develop Kirkendall porosity. An attempt by the Cu<sub>3</sub>Sn layer to sustain its thickness was evidenced by its apparent, localized accelerated growth (plumes) into the Cu substrate.

The driving force for accelerated growth by the Cu<sub>6</sub>Sn<sub>5</sub> layer in the 95.5Sn-3.9Ag-0.6Cu/Cu couples aged at 205°C was apparently absent in the other Pb-free solder/Cu couples. The differences in Cu and Ag contents did not provide a consistent explanation for an anomalous Cu<sub>6</sub>Sn<sub>5</sub> growth via a *chemical potential* effect. On the other hand, an alternative driving force may have been the solder-field microstructure. Phase distributions as well as the presence of point and line defects in the 95.5Sn-3.9Ag-0.6Cu solder that were sensitive to the aging treatments, could have enhanced Sn diffusion to the solder/IMC layer interface and, thus, accelerated Cu<sub>6</sub>Sn<sub>5</sub> layer growth.

Evidence of a possible microstructural driving force was indicated when the more extensively grown IMC layer encountered coarsened Ag<sub>3</sub>Sn particles in the solder. The Ag<sub>3</sub>Sn particles acted as physical barriers to the IMC (actually the Cu<sub>6</sub>Sn<sub>5</sub> layer) growth. The micrograph in Fig. 11 shows the bowed interface between the IMC layer and the 95.5Sn-3.9Ag-0.6Cu solder of the sample aged at 205°C for 50 days. The interface bow indicates that the Sn/Ag<sub>3</sub>Sn interface of the particles did not ap-

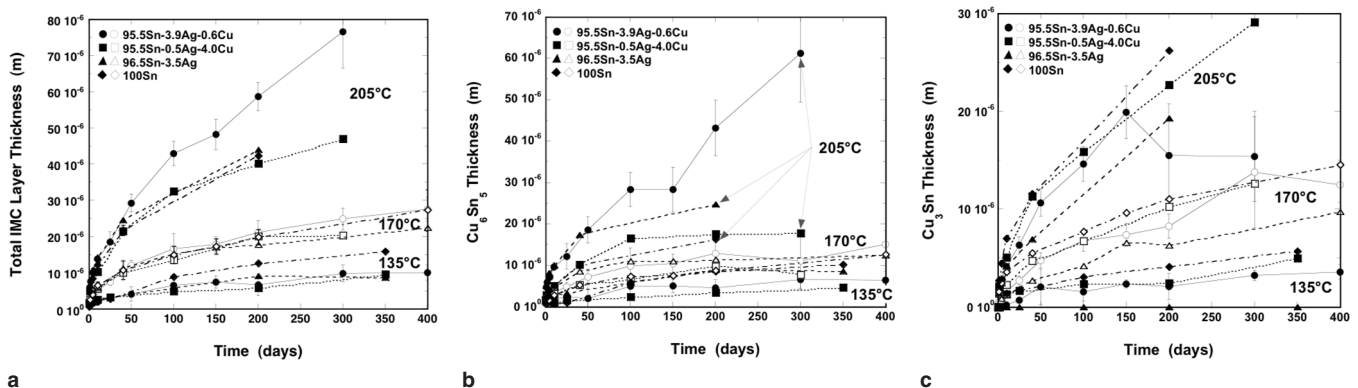


Fig. 10. Solid-state IMC thickness as a function of aging time for each of the Pb-free solder couples for aging temperatures of 135°C, 170°C, and 205°C: (a) total IMC layer, (b) Cu<sub>6</sub>Sn<sub>5</sub> layer, and (c) Cu<sub>3</sub>Sn layer. Alloy compositions were distinguished by symbol shape and line format. Solid symbols represented the 135°C and 205°C data; open symbols represented the 170°C data.

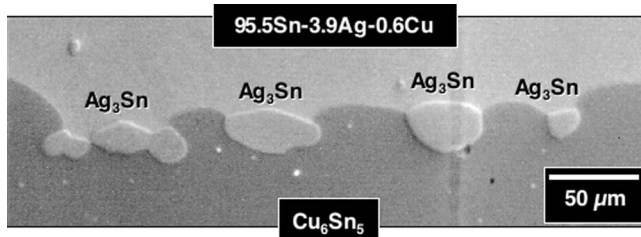


Fig. 11. The SEM photograph showing the pinning of the IMC ( $\text{Cu}_6\text{Sn}_5$ ) layer front by coarsened  $\text{Ag}_3\text{Sn}$  particles in the 95.5Sn-3.9Ag-0.6Cu solder. The aging conditions were 170°C, 200 days.

parently provide a short-circuit diffusion path that would accelerate IMC growth there. Rather, the opposite occurred; IMC growth was reduced along the Sn/ $\text{Ag}_3\text{Sn}$  interface. It was concluded that Sn diffusion toward the solder/IMC interface would be enhanced by the presence of fewer  $\text{Ag}_3\text{Sn}$  particles. The number of  $\text{Ag}_3\text{Sn}$  particles was reduced by coarsening, particularly so at the highest aging temperatures, thereby providing the driving force that accelerated IMC ( $\text{Cu}_6\text{Sn}_5$ ) growth to an extent that caused the observed porosity.

Coincidentally, the 96.5Sn-3.5Ag solder has a microstructure that was similar to that of the 95.5Sn-3.9Ag-0.6Cu solder. Yet, 96.5Sn-3.5Ag/Cu couples did not exhibit an accelerated  $\text{Cu}_6\text{Sn}_5$  layer growth and porosity phenomena. It can only be assumed that the presence of 0.6 wt.% and a reduced eutectic temperature of the ternary alloy also had a role in the IMC layer growth behavior. Clearly, the hypothesis of a microstructural driving force is far from conclusive.

### Electron Probe Microanalysis: The IMC Layer Composition

The  $\text{Cu}_3\text{Sn}$  and  $\text{Cu}_6\text{Sn}_5$  stoichiometries were confirmed to have developed in the solid-state aging of 100Sn/Cu, 96.5Sn-3.5Ag/Cu, 95.5Sn-0.5Ag-4.0Cu/Cu, and 63Sn-37Pb/Cu couples.<sup>3,4,7</sup> The singular exception was the intermittent occurrence of  $\text{CuSn}$  in the IMC layer of a 96.5Sn-3.5Ag/Cu couple aged at 205°C for 100 days. The corresponding EPMA trace is shown in Fig. 12. Because  $\text{CuSn}$  is not identified in the equilibrium Cu-Sn binary-alloy phase diagram, it was likely a metastable variant of the  $\text{Cu}_6\text{Sn}_5$  compound.<sup>11</sup>

The EPMA technique confirmed the nominal  $\text{Cu}_6\text{Sn}_5$  and  $\text{Cu}_3\text{Sn}$  (when present) stoichiometries in the 95.5Sn-3.9Ag-0.6Cu/Cu couples for all aging conditions. The general interface morphology of 95.5Sn-3.9Ag-0.6Cu/Cu couples was represented by the EPMA trace shown in Fig. 13a for the specimen aged at 205°C for 50 days. The corresponding location of the trace was indicated by the SEM image in Fig. 13b. Small concentration gradients of Cu and Sn were observed in both  $\text{Cu}_6\text{Sn}_5$  and  $\text{Cu}_3\text{Sn}$  layers having Cu and Sn concentrations that decreased and increased, respectively, from the Cu substrate to the solder field. The gradients were slightly steeper for Cu than for Sn.

The EPMA trace in Fig. 13a intercepted an Ag-Sn particle located at the  $\text{Cu}_6\text{Sn}_5$ /solder interface. It

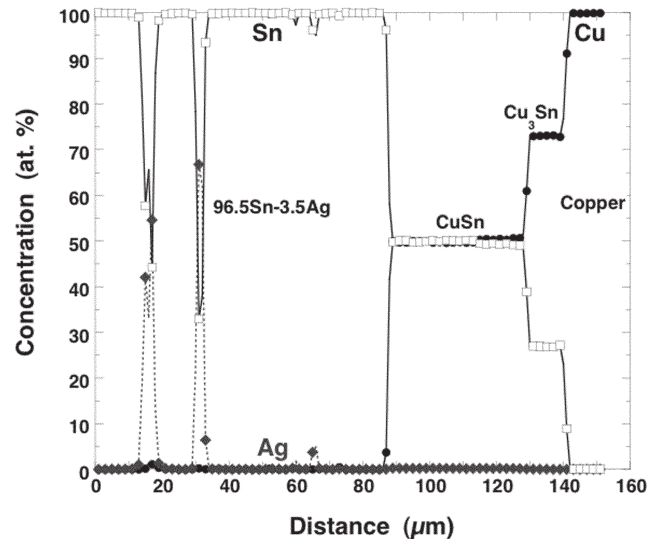


Fig. 12. The EPMA evaluation of the 96.5Sn-3.5Ag/Cu couple aged at 205°C for 100 days showing the  $\text{CuSn}$  that occurred in four of six traces.

was not possible to determine whether a trace of Cu was actually present in the particle or was an artifact of the layer geometry and EPMA sampling-volume effect. At this juncture, the particle composition was designated as  $\text{Ag}_3\text{Sn}$ .

The EPMA technique indicated no unusual behavior in couples aged at 70°C, 100°C, 135°C, or 170°C. Therefore, the discussion will concentrate on those couples aged at 205°C and, specifically, aging times greater than 150 days. These couples exhibited the interface porosity and accelerated  $\text{Cu}_3\text{Sn}$  growth (Fig. 9). Shown in Fig. 14 is the EPMA trace and SEM photograph of the IMC layer in the couple aged at 205°C for 200 days. Porosity had begun to develop at the  $\text{Cu}_3\text{Sn}$ /Cu interface (Fig. 14b). The  $\text{Cu}_6\text{Sn}_5$  and  $\text{Cu}_3\text{Sn}$  layers exhibited the gradients of both Cu and Sn as were noted above.

The EPMA trace in Fig. 14 passed through an  $\text{Ag}_3\text{Sn}$  particle contained within the  $\text{Cu}_6\text{Sn}_5$  layer. There was 1–2at.%Cu contained in the particle. Similar arguments of particle depth and sampling-volume effects that were made previously could explain the presence of Cu in this particle. However, it was an unexpected coincidence. Therefore, it was possible that the  $\text{Ag}_3\text{Sn}$  particles in Figs. 13 and 14 indeed contained a trace of Cu. The Ag-Cu equilibrium phase diagram indicates a limited solubility for Cu in Ag.<sup>12</sup>

The EPMA was performed on the 95.5Sn-3.9Ag-0.6Cu/Cu couple aged at 205°C for 400 days. This sample exhibited a great deal of porosity in the  $\text{Cu}_3\text{Sn}$  layer and along the  $\text{Cu}_3\text{Sn}$ /Cu interface. The EPMA elemental trace and SEM photograph of the trace location are shown in Fig. 15a and b, respectively. The analysis confirmed the local growth of the  $\text{Cu}_3\text{Sn}$  layer into the Cu substrate. That growth plume was not homogeneously  $\text{Cu}_3\text{Sn}$  because there remained small regions of elemental Cu.



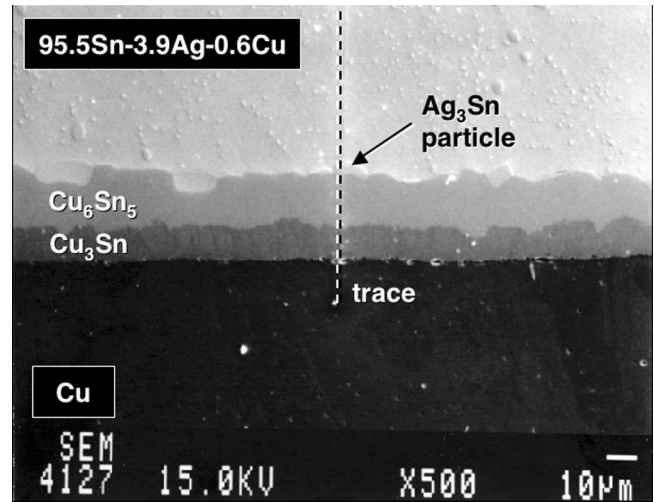
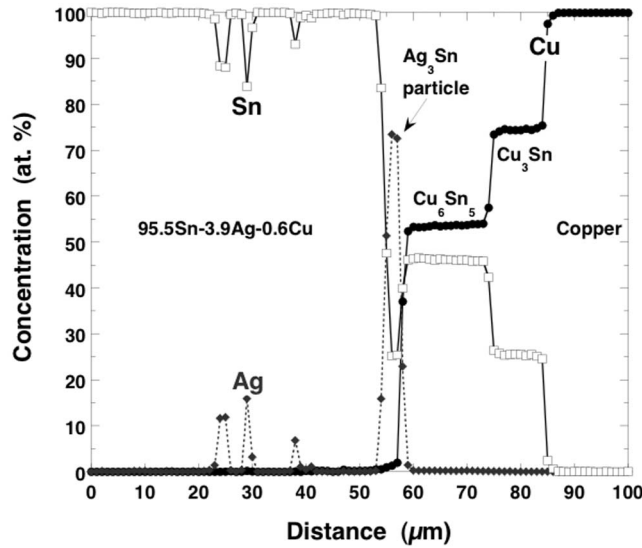


Fig. 13. (a) The EPMA evaluation of the 95.5Sn-3.9Ag-0.6Cu/Cu couple aged at 205°C for 50 days. (b) An SEM photograph showing the location of the EPMA trace.

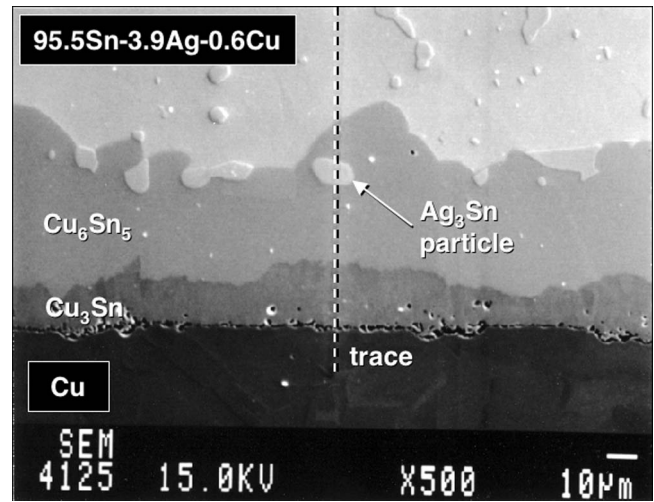
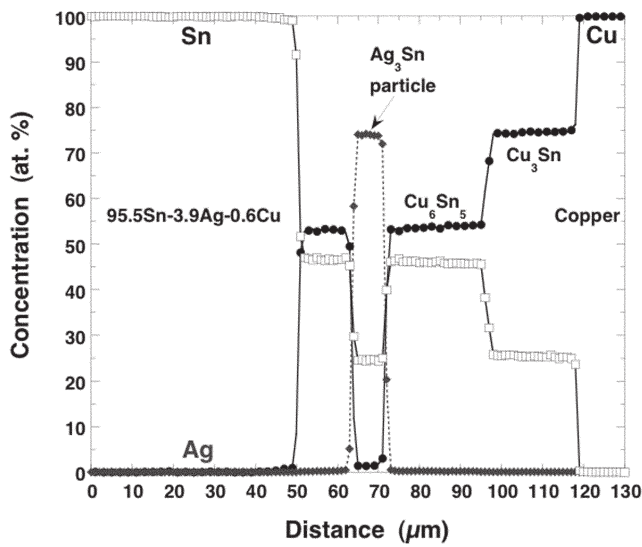


Fig. 14. (a) The EPMA evaluation of the 95.5Sn-3.9Ag-0.6Cu/Cu couple aged at 205°C for 200 days. (b) An SEM photograph showing the location of the EPMA trace.

In summary, the EPMA determined that the  $\text{Cu}_6\text{Sn}_5$  and  $\text{Cu}_3\text{Sn}$  stoichiometries comprised the IMC layer in 95.5Sn-3.9Ag-0.6Cu/Cu couples exposed to solid-state aging. The coarsened  $\text{Ag}_3\text{Sn}$  particles intercepted by the advancing IMC layer may have contained a trace amount of Cu (1–2 at.%). The EPMA study also confirmed the localized, accelerated growth of  $\text{Cu}_3\text{Sn}$  into the Cu substrate that accompanied porosity development when the couples were aged at 205°C for times of 300–400 days.

#### Electron Probe Microanalysis: The Near-Interface Solder Field

The EPMA traces were extended a distance of 40–80  $\mu\text{m}$  into the solder field beyond the solder/IMC

interface. This added evaluation was performed to determine (1) whether there was excess Cu in the solder (beyond the 1 at.% from the nominal solder composition) caused by substrate dissolution and (2) the impact that additional Cu, if present, had on solid-state IMC layer growth. First, the EPMA data will be presented; then, a summarization will be made of those results.

Shown in Fig. 16a is the EPMA trace obtained from the 95.5Sn-3.9Ag-0.6Cu/Cu couple aged at 70°C for 25 days. This case was also representative of the as-fabricated condition. The broad Ag peaks represent the interdendritic ternary eutectic regions comprised of aggregates of small  $\text{Ag}_3\text{Sn}$  particles and Cu in a Sn-rich matrix phase. The EPMA could

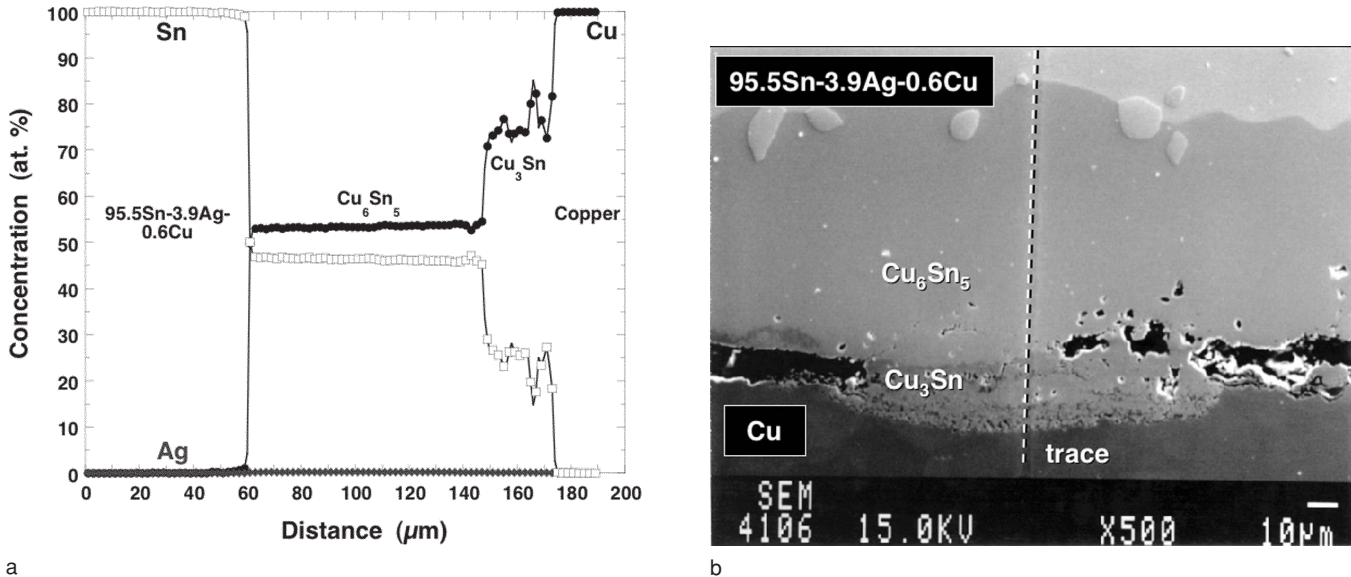


Fig. 15. (a) The EPMA evaluation of the 95.5Sn-3.9Ag-0.6Cu/Cu couple aged at 205°C for 400 days. (b) An SEM photograph showing the location of the EPMA trace.

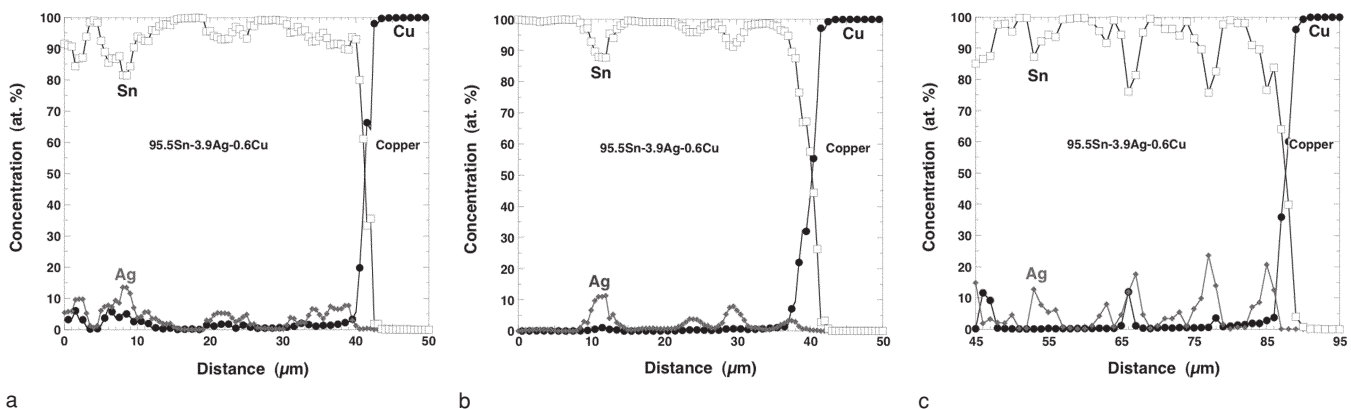


Fig. 16. The EPMA traces showing the near-interface solder-field composition of samples aged under the following conditions: (a) 70°C, 25 days; (b) 70°C, 200 days; and (c) 100°C, 200 days.

not resolve the individual  $\text{Ag}_3\text{Sn}$  particles. Several regions of  $\text{Ag}_3\text{Sn}$  particles were accompanied by elevated concentrations of Cu. The peak Cu concentrations were generally 3–5 at.%; however, a few locations had Cu concentrations as high as 8–10 at.%. It was hypothesized that the Cu was present as either small Cu-Sn IMC particles or as a trace element in the  $\text{Ag}_3\text{Sn}$  particles—a  $(\text{Ag,Cu})_x\text{Sn}_y$  stoichiometry. Copper was *not* detected in the Sn-rich dendritic structures within the solder.

A Cu concentration gradient was observed at the solder/IMC interface. The Cu level decreased from approximately 3 at.% to 0 at.% over a distance of 10  $\mu\text{m}$ , going from the IMC/solder interface into the solder field. This Cu gradient was observed when a ternary eutectic region or Sn-rich dendrite regions were present at the interface. This Cu gradient was not a “smearing” artifact caused by the metallographic sample-preparation process.

The EPMA trace taken across the 95.5Sn-3.9Ag-0.6Cu/Cu couple that was aged at 70°C for 200 days

is shown in Fig. 16b. Relatively shallow Cu peaks were associated with aggregates of  $\text{Ag}_3\text{Sn}$  particles that had, as yet, exhibited negligible coarsening. The Cu concentration gradient had diminished at the solder/IMC interface; the Cu level decreased from approximately 1–2 at.% to 0 at.% over 5  $\mu\text{m}$ .

The Cu peaks became more numerous in couples aged at 100°C for 200 days (Fig. 16c), which was concurrent with coarsening of the  $\text{Ag}_3\text{Sn}$  particles. The Cu concentration gradient at the solder/IMC interface decreased from 3–4 at.% to 0 at.% over distances of 5–10  $\mu\text{m}$ . Similar EPMA traces were recorded for the couple aged at 100°C for 400 days.

The EPMA evaluations of 95.5Sn-3.9Ag-0.6Cu/Cu couples aged at 135°C and 170°C were limited to those couples aged for 200 days. Those traces showed an absence of detectable Cu in the solder field. Copper concentration gradients were observed at the solder/IMC interface with Cu levels decreasing from 3–4 at.% to 0 at.% over 10  $\mu\text{m}$  at 135°C and from 1–2 at.% to 0 at.% over 5  $\mu\text{m}$  at 170°C.

Similarly, the EPMA evaluation of couples aged at 205°C for 10 days, 50 days, 200 days, or 400 days did not detect a measurable Cu signal in the solder field. A Cu concentration gradient persisted at the solder/IMC layer interface; the Cu signal decreased from 1–2 at.% to 0 at.% over a distance of 5–10  $\mu\text{m}$  from the interface into the solder field.

The behavior of Cu in the near-interface solder field was also evaluated for the 95.5Sn-0.5Ag-4.0Cu/Cu, 100Sn/Cu, and 96.5Sn-3.5Ag/Cu couples. In the case of the 95.5Sn-0.5Ag-4.0Cu/Cu couples, it was not possible to distinguish Cu present in the solder that did not originate from the nominal solder composition. Copper was present as stand alone  $\text{Cu}_6\text{Sn}_5$  particles and in association with the Ag signal when solid-state aging was very minimal. Further aging resulted in *only* the presence of a few  $\text{Cu}_6\text{Sn}_5$  particles; that is, Cu was no longer associated with the coarsened  $\text{Ag}_3\text{Sn}$  particles, which is similar to trends observed in the 95.5Sn-3.9Ag-0.6Cu/Cu couples. The 95.5Sn-0.5Ag-4.0Cu/Cu couples exhibited a Cu concentration gradient from the solder/IMC interface into the solder that went from 4 at.% to 0 at.% over a 20- $\mu\text{m}$  distance when aged at 100°C for 25 days and 350 days. Increasing the aging temperature to 170°C (200 days) and 205°C (10 days and 300 days) decreased the gradient; the Cu content dropped from 1 at.% to 0 at.% over a distance of 5–10  $\mu\text{m}$ .

The 100Sn/Cu couples aged at 170°C (40 days) and 205°C (4 days and 40 days) exhibited only a presence of isolated  $\text{Cu}_6\text{Sn}_5$  particles in the solder that originated from Cu dissolved from the substrate. There were negligible Cu-concentration gradients detected at the solder/IMC layer interface.

The 96.5Sn-3.5Ag/Cu couples were also evaluated. The as-fabricated 96.5Sn-3.5Ag/Cu couples exhibited Cu concentrations in the interdendritic regions [ $\text{Ag}_3\text{Sn}$  particles + Sn]. Clearly, the source of the Cu was dissolution of the substrate material. Those areas of elevated Cu concentration remained after aging at 70°C for 100 days but then decreased slightly after 300 days. These trends were similar to those of the 95.5Sn-3.9Ag-0.6Cu/Cu couples.

Aging the 96.5Sn-3.5Ag/Cu couples at 100°C for 300 days resulted in the appearance of isolated Cu peaks among the  $\text{Ag}_3\text{Sn}$  particles. The aging conditions of 135°C and 100 days as well as 135°C and 300 days resulted in Cu being present only as  $\text{Cu}_6\text{Sn}_5$  particles among the coarsened  $\text{Ag}_3\text{Sn}$  particles.

The 96.5Sn-3.5Ag/Cu couples were evaluated after aging at 170°C for 4 days, 40 days, 100 days, and 300 days. Despite a solder microstructure after 4 days that was very similar to the as-fabricated condition (i.e., aggregates of  $\text{Ag}_3\text{Sn}$  particles in the interdendritic, Sn-rich matrix), copper was present in the interdendritic region as one or two, small Cu peaks. The longer aging times of 40–300 days resulted in further coarsening of  $\text{Ag}_3\text{Sn}$  particles, several of which contained a trace of Cu (1 at.%). Otherwise, there was no other presence of Cu in the 96.5Sn-3.5Ag solder, not even as  $\text{Cu}_6\text{Sn}_5$  particles.

The 96.5Sn-3.5Ag/Cu couples were also evaluated by EPMA after aging at 205°C for 4 days, 25 days, 40 days, 100 days, and 300 days. Aging for 4 days resulted in the same observations as were recorded previously for aging at 170°C. Aging at 25 days through 300 days resulted in only a few, small isolated regions having a trace of Cu (<1 at.%). Otherwise, the microstructures contained primarily coarsened  $\text{Ag}_3\text{Sn}$  particles.

The 96.5Sn-3.5Ag/Cu couples did not exhibit a Cu concentration gradient at the solder/IMC interface, a point that was in contrast to the 95.5Sn-3.9Ag-0.6Cu/Cu couples.

In summary, EPMA studies of the as-fabricated 95.5Sn-3.9Ag-0.6Cu/Cu couples indicated a presence of Cu in the near-interface solder field. At the levels observed and their (albeit, one-dimensional) distribution, it could not be determined, conclusively, whether the source of the Cu peaks was dissolution of the Cu substrate or were areas where Cu from the solder composition had simply become concentrated. The Cu peaks were associated with the  $\text{Ag}_3\text{Sn}$  particles in the interdendritic regions. A similar phenomenon was observed in the near-interface solder fields of the 96.5Sn-3.5Ag/Cu couples. However, in this case, the source of the additional Cu was clearly dissolution of the Cu substrate.

An increase of solid-state aging caused a gradual loss of the Cu from the solder fields of the 95.5Sn-3.9Ag-0.6Cu/Cu and 96.5Sn-3.5Ag/Cu couples. A similar process was observed with the  $\text{Ag}_3\text{Sn}$  particles of the 95.5Sn-0.5Ag-4.0Cu/Cu couples. Based upon the 96.5Sn-3.5Ag/Cu couples, it would be surmised that the Cu diffused back to the solder/IMC interface, likely contributing to the development of the IMC layer, albeit, to a relatively minimal extent given the overall amount of Cu present in the solder. At this point, it can only be inferred from the similar trends with aging that the same process occurred in the 95.5Sn-3.9Ag-0.6Cu/Cu couples, assuming that the Cu peaks in Fig. 16a were, indeed, the result of excess Cu caused by substrate dissolution.

Last, a Cu concentration gradient developed at the solder/IMC interface of the 95.5Sn-3.9Ag-0.6Cu/Cu couples. The fact that those gradients diminished with the increased solid-state aging, which was coincidental with the loss of Cu from the solder field, suggested that the gradients were a result of Cu diffusion from the solder field to the IMC layer. On the other hand, an absence of significant gradients at the solder/IMC layer interface of 96.5Sn-3.5Ag/Cu couples indicates that the gradient is not a necessary effect of the Cu movement from the solder to the IMC layer.

#### IMC Layer Growth Kinetics in 95.5Sn-3.9Ag-0.6Cu/Cu Couples

The IMC layer thickness,  $x$  (m), as a function of solid-state aging time,  $t$  (sec), and temperature,  $T$  (K), is predicted by Eqs. 3–5 for the  $\text{Cu}_3\text{Sn}$  layer, the  $\text{Cu}_6\text{Sn}_5$  layer, and the total IMC layer, respectively.

The error terms represent a 95% confidence interval for each mean value.

$$\text{Cu}_3\text{Sn} \quad x = 5.91 \times 10^{-4} t^{0.56 \pm 0.06} \exp[(-50 \pm 6 \text{ kJ/mol})/RT] \quad (3)$$

$$\text{Cu}_6\text{Sn}_5 \quad x = 0.9 \pm 0.3 \times 10^{-6} + 2.64 \times 10^{-4} t^{0.54 \pm 0.07} \exp[(-44 \pm 4 \text{ kJ/mol})/RT] \quad (4)$$

$$\text{Total} \quad x = 0.9 \pm 0.3 \times 10^{-6} + 1.05 \times 10^{-3} t^{0.58 \pm 0.07} \exp[(-50 \pm 4 \text{ kJ/mol})/RT] \quad (5)$$

The values of the square of the correlation coefficient,  $R^2$ , for Eqs. 3–5 were 0.95, 0.93, and 0.95, respectively, which indicated excellent correlation over the aging temperature range. The time exponent values were statistically the same between all three equations, indicating that diffusion was the active mechanism.<sup>9</sup> The apparent-activation energy values were also the same between the three equations. Those values of 40–60 kJ/mol suggested that a fast or “short-circuit” diffusion path, such as grain boundary diffusion within the IMC layer, was responsible for the latter’s development.<sup>10</sup>

### IMC Layer Growth Kinetics Versus Solder Composition

A comparison was made of the IMC layer growth kinetics between the 95.5Sn-3.9Ag-0.6Cu/Cu couples and the other Pb-free solder compositions, beginning with the  $\text{Cu}_3\text{Sn}$  layer. As noted previously, the 95.5Sn-3.9Ag-0.6Cu/Cu couples, like the 96.5Sn-3.5Ag/Cu couples, required higher aging temperatures to develop a  $\text{Cu}_3\text{Sn}$  layer as compared to the 100Sn/Cu and 95.5Sn-0.5Ag-4.0Cu/Cu couples (Table I). A comparison is made of  $n$  and  $\Delta H$  values as a function of solder composition for  $\text{Cu}_3\text{Sn}$  growth in Fig. 17. The 95.5Sn-3.9Ag-0.6Cu/Cu and 96.5Sn-3.5Ag/Cu couples exhibited similar values of  $n$  that were nearly equal to 0.5. On the other hand, the 100Sn/Cu and 95.5Sn-0.5Ag-4.0Cu/Cu couples had similar, yet significantly lower, time exponent val-

ues, suggesting that diffusion may not have been the rate-controlling mechanism in these couples. Rather, interface reactions may have become important to the IMC layer growth process.

The apparent-activation energy,  $\Delta H$ , of  $\text{Cu}_3\text{Sn}$ -layer growth exhibited similar trends as a function of solder composition (Fig. 17). The 95.5Sn-3.9Ag-0.6Cu/Cu and 96.5Sn-3.5Ag/Cu couples had higher, yet statistically the same, values of  $\Delta H$ . The 100Sn/Cu and 95.5Sn-0.5Ag-4.0Cu/Cu couples had lower apparent-activation energies that were in the range of 20–30 kJ/mol, which further substantiated the likelihood that an alternative mechanism also contributed to layer growth.

The growth behavior of the  $\text{Cu}_3\text{Sn}$  layer was similar between the 95.5Sn-3.9Ag-0.6Cu/Cu and 96.5Sn-3.5Ag/Cu couples. Two hypotheses are proposed to explain this similarity. (a) The mere presence of Ag or the lower solidus temperature caused by the Ag constituent, affected  $\text{Cu}_3\text{Sn}$ -layer growth. (b) Silver indirectly affected  $\text{Cu}_3\text{Sn}$ -layer development by altering the solder microstructure via the  $\text{Ag}_3\text{Sn}$  particles. The similar  $\text{Cu}_3\text{Sn}$ -layer growth between the 100Sn/Cu and 95.5Sn-0.5Ag-4.0Cu/Cu couples appears to result from the absence of significant Ag content in the solders. Moreover, the latter two couples indicated that the nominal Cu content of the solder was not a significant factor in the  $\text{Cu}_3\text{Sn}$ -layer growth kinetics.

The  $\text{Cu}_6\text{Sn}_5$  layer developed in the as-fabricated condition of all couples. It was noted earlier that the initial thickness of  $0.9 \pm 0.3 \times 10^{-6}$  m observed in the 95.5Sn-3.9Ag-0.6Cu/Cu couples was comparable to that of the 100Sn/Cu couples and approximately one-half of thicknesses observed in the 96.5Sn-3.5Ag/Cu and 95.5Sn-0.5Ag-4.0Cu/Cu couples (Table III). It is important to recognize that the as-fabricated  $\text{Cu}_6\text{Sn}_5$  layers developed when the solders were in the *liquid state* and, as such, resulted from interface reaction/diffusion processes that are different from those active during solid-state growth.

The  $\text{Cu}_6\text{Sn}_5$  layer growth-kinetics parameters  $n$  and  $\Delta H$  were plotted as a function of solder composition in Fig. 18. Unlike the kinetics parameters for the  $\text{Cu}_3\text{Sn}$  layer, neither  $n$  nor  $\Delta H$  exhibited a statistically significant dependence upon the Pb-free solder composition. The lower mean value of  $\Delta H$  for the 100Sn/Cu couples was accompanied by a larger confidence interval that precluded there from being a statistical significance to this trend. The values of  $n$  and  $\Delta H$  indicated that a fast-diffusion process was largely responsible for layer growth.

Last, the values of  $n$  and  $\Delta H$  representing the total IMC layer growth were plotted as a function of solder composition in Fig. 19. It was clear that the growth kinetics of the total IMC layer thickness reflected largely those of the  $\text{Cu}_6\text{Sn}_5$  layer.

In summary, a comparison was made of the IMC layer growth kinetics between the four Pb-free solder/Cu couples. Only the kinetics of  $\text{Cu}_3\text{Sn}$  growth

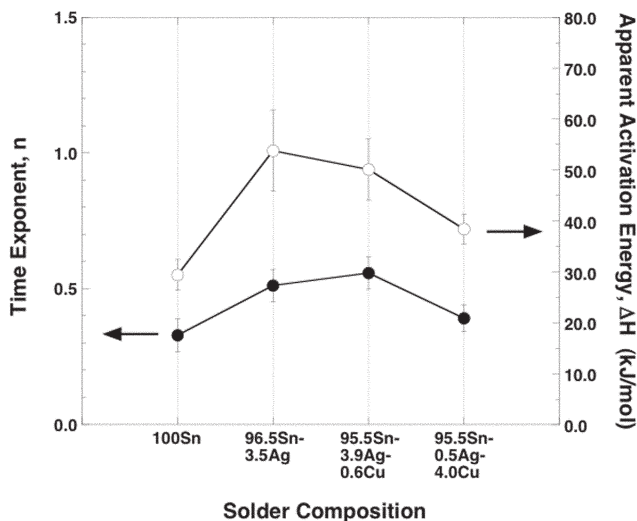


Fig. 17. Graph of the time exponent,  $n$ , and apparent-activation energy,  $\Delta H$ , for  $\text{Cu}_3\text{Sn}$ -layer growth as a function of solder composition.

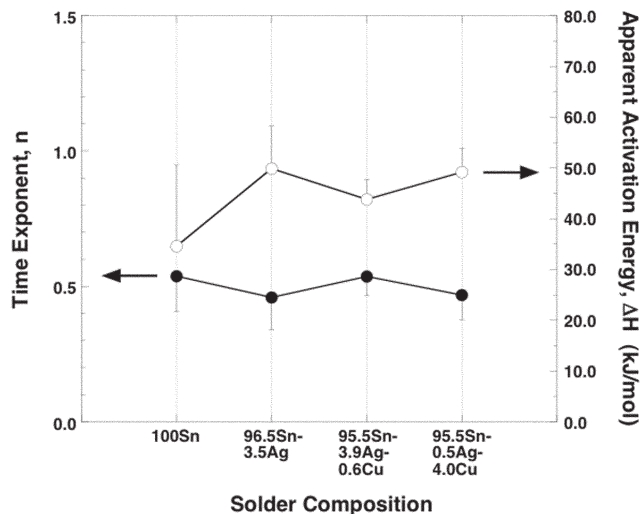


Fig. 18. Graph of the time exponent,  $n$ , and apparent-activation energy,  $\Delta H$ , for  $\text{Cu}_6\text{Sn}_5$  layer growth as a function of solder composition.

were sensitive to the solder composition and, specifically, the Ag component of those compositions. Development of the  $\text{Cu}_6\text{Sn}_5$  layer, which also dominated the total IMC layer growth kinetics, was not sensitive to the solder composition. These trends, together with observations that the total IMC layer thicknesses were comparable between the four solder/Cu couples as a function of aging time and temperature, provides additional evidence that the primary effect of solder composition on solid-state IMC layer growth is in the thickness fraction and growth kinetics of the  $\text{Cu}_3\text{Sn}$  layer. (The initial indications to this behavior were observed in a comparison of solid-state IMC layer growth between 100Sn/Cu and 63Sn-37Pb/Cu couples.<sup>4</sup>)

### SUMMARY

- Long-term, solid-state IMC layer growth was examined in couples of the Pb-free solder, 95.5 Sn-3.9Ag-0.6Cu (wt.%), and copper (Cu). Aging temperatures ranged from 70°C to 205°C; aging times were 1–400 days. The IMC layer growth properties were compared to those of the 96.5 Sn-3.5Ag/Cu, 95.5Sn-0.5Ag-4.0Cu/Cu, and 100Sn/Cu couples that were determined in previous studies.
- The EPMA identified the nominal  $\text{Cu}_3\text{Sn}$  and  $\text{Cu}_6\text{Sn}_5$  stoichiometries within the IMC layer. When present, the  $\text{Cu}_3\text{Sn}$  layer comprised 0.4–0.6 of the total layer thickness. Copper and Sn concentration gradients were observed in each layer stoichiometry.
- The  $\text{Cu}_3\text{Sn}$  and  $\text{Cu}_6\text{Sn}_5$  layer thicknesses in 95.5Sn-3.9Ag-0.6Cu/Cu couples were similar to those in the other solder/Cu couples at aging temperatures of 70–170°C. However, aging at 205°C and times greater than 150 days caused an accelerated growth of the  $\text{Cu}_6\text{Sn}_5$  layer in 95.5Sn-3.9Ag-0.6Cu/Cu couples that was accompanied by porosity development at the  $\text{Cu}_3\text{Sn}/\text{Cu}$

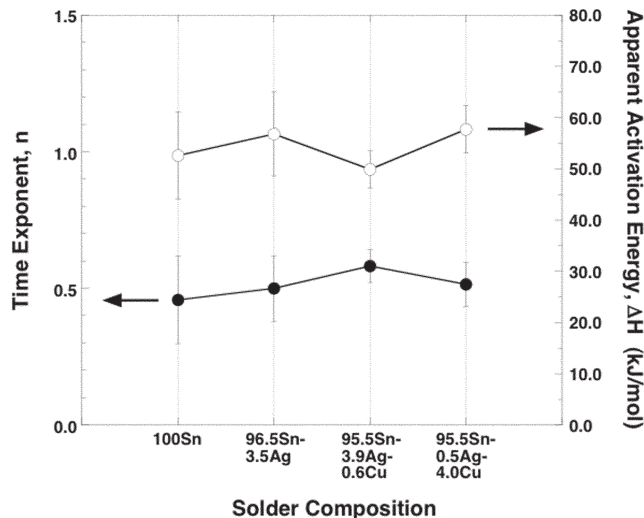


Fig. 19. Graph of the time exponent,  $n$ , and apparent-activation energy,  $\Delta H$ , for the total IMC layer ( $\text{Cu}_3\text{Sn} + \text{Cu}_6\text{Sn}_5$ ) growth as a function of solder composition.

interface and in the  $\text{Cu}_3\text{Sn}$  layer as well as localized plumes of accelerated growth by the  $\text{Cu}_3\text{Sn}$  layer into the Cu substrate.

- Coarsened  $\text{Ag}_3\text{Sn}$  particles in the solder field appeared to pose only physical obstacles to the advancing IMC ( $\text{Cu}_6\text{Sn}_5$ ) layer of 95.5Sn-3.9Ag-0.6Cu/Cu couples.
- The EPMA identified an excess of Cu at 3–5 at.% and as high as 8 at.% associated with the  $\text{Ag}_3\text{Sn}$  particles of the near-interface 95.5Sn-3.9Ag-0.6Cu solder field. A Cu gradient was also observed in the solder, leading up to the IMC layer. The excess Cu and interface Cu gradient diminished with solid-state aging, suggesting that the Cu contributed to IMC layer growth. A similar behavior was observed in 96.5Sn-3.5Ag/Cu couples.
- The growth kinetics of the IMC layer in 95.5Sn-3.9Ag-0.6Cu/Cu couples were described by the equation  $x = x_0 + At^n \exp[\Delta H/RT]$ . The time exponents,  $n$ , were  $0.56 \pm 0.06$ ,  $0.54 \pm 0.07$ , and  $0.58 \pm 0.07$  for the  $\text{Cu}_3\text{Sn}$  layer, the  $\text{Cu}_6\text{Sn}_5$ , and the total IMC layer, respectively. The apparent-activation energies ( $\Delta H$ ) were  $\text{Cu}_3\text{Sn}$  layer:  $50 \pm 6$  kJ/mol;  $\text{Cu}_6\text{Sn}_5$  layer:  $44 \pm 4$  kJ/mol; and total layer:  $50 \pm 4$  kJ. The values of  $n$  and  $\Delta H$  indicated that a fast-diffusion mechanism was active. When included with similar data from other Pb-free solder/Cu couples, it was apparent that the  $\text{Cu}_3\text{Sn}$  growth kinetics were sensitive to solder composition while those of  $\text{Cu}_6\text{Sn}_5$  layer growth, which also dominated the rate kinetics of total layer development, were insensitive to solder composition.

### ACKNOWLEDGEMENTS

The authors thank R. Wright and G. Bryant for preparation of the metallographic cross-section samples and M. Dvorack for his comments and thorough review of this manuscript. Sandia is a

multiprogram laboratory operated by Sandia Corporation, a Lockheed Martin Company, for the United States Department of Energy's National Nuclear Security Administration under Contract No. DE-AC04-94AL85000.

### REFERENCES

1. P. Vianco, *Soldering Surf. Mount Technol.* 14, 26 (2002).
2. P. Vianco, in *Handbook of Lead (Pb)-Free Technology for Microelectronic Assembly* (New York: Marcel-Dekker, 2004), pp. 167–210.
3. P. Vianco, P. Hlava, and A. Kilgo, *J. Electron. Mater.* 23, 583 (1994).
4. P. Vianco, K. Erickson, and P. Hopkins, *J. Electron. Mater.* 23, 721 (1994).
5. P. Vianco, A. Kilgo, and R. Grant, *J. Electron. Mater.* 24, 1493 (1995).
6. P. Vianco and J. Rejent, *J. Electron. Mater.* 28, 1131 (1999).
7. P. Vianco, P. Hlava, A. Kilgo, and J. Rejent, in *Environmentally Friendly Electronics—Lead Free Technology*, ed. J. Hwang (Ayr, UK: Electrochem Pub. Ltd., 2001) pp. 436–483.
8. P. Vianco, *Soldering Handbook*, 3rd ed. (Miami, FL: American Welding Society, 2000), p. 91.
9. E. Machlin, *An Introduction to Aspects of Thermodynamics and Kinetics Relevant to Material Science* (New York: McGraw-Hill, 1991), pp. 190–192.
10. P. Shewmon, *Diffusion in Solids* (Warrendale, PA: TMS, 1989), pp. 191–202.
11. T. Massalski, ed., *Binary Alloy Phase Diagrams*, Vol. 1 (Materials Park, OH: ASM, 1986), p. 965.
12. T. Massalski, ed., *Binary Alloy Phase Diagrams*, Vol. 1 (Materials Park, OH: ASM, 1986), p. 19.